Journal of Macromolecular Science, Part A
Publication details, including instructions for authors and subscription information:
http://www.informaworld.com/smpp/title~content=t713597274

Evaluation of Biocompatible Photopolymers I: Photoreactivity and Mechanical Properties of Reactive Diluents

M. Schuster[a]; C. Turecek[b]; B. Kaiser[c]; J. Stampfl[c]; R. Liska[a]; F. Varga[b]
[a] Institute of Applied Synthetic Chemistry - Division of Macromolecular Chemistry, Vienna University of Technology, Vienna, Austria [b] Ludwig Boltzmann Institute of Osteology at the Hanusch Hospital of WGKK and AUVA Trauma Centre Meidling, 4th Medical Department, Vienna, Austria [c] Institute of Materials Science and Technology, Vienna University of Technology, Vienna, Austria

Online publication date: 13 October 2010

To cite this Article Schuster, M. , Turecek, C. , Kaiser, B. , Stampfl, J. , Liska, R. and Varga, F.(2007) 'Evaluation of Biocompatible Photopolymers I: Photoreactivity and Mechanical Properties of Reactive Diluents', Journal of Macromolecular Science, Part A, 44: 5, 547 — 557
To link to this Article: DOI: 10.1080/10601320701235958
URL: http://dx.doi.org/10.1080/10601320701235958

Journal of Macromolecular Science ®, Part A: Pure and Applied Chemistry (2007) **44**, 547–557

ISSN: 1060-1325 print/1520-5738 online
DOI: 10.1080/10601320701235958

Evaluation of Biocompatible Photopolymers I: Photoreactivity and Mechanical Properties of Reactive Diluents

M. SCHUSTER,[1] C. TURECEK,[2] B. KAISER,[3] J. STAMPFL,[3] R. LISKA,[1] and F. VARGA[2]

[1]*Institute of Applied Synthetic Chemistry – Division of Macromolecular Chemistry, Vienna University of Technology, Vienna, Austria*
[2]*Ludwig Boltzmann Institute of Osteology at the Hanusch Hospital of WGKK and AUVA Trauma Centre Meidling, 4th Medical Department, Vienna, Austria*
[3]*Institute of Materials Science and Technology, Vienna University of Technology, Vienna, Austria*

Received August, 2006, Accepted December, 2006

Important characteristics of bone replacement materials are to support the attachment, growth, and differentiation of osteogenic cells. A second important characteristic of the material is that it can be photopolymerized, which allows the material to be applied to rapid prototyping that enables us to fabricate scaffolds in nearly any shape and structure. In these investigations, reactivity and biocompatibility of different types of commercially available acrylates and photoinitiators were determined. Cell viability was related to the functional groups in the monomers present, e.g., oligoethyleneglycol, urethane-, hydroxy- or carboxy groups. It was found that polymers obtained from acrylates with urethane units, most dialkylacrylamide and especially trimethylolpropane triacrylate gave outstanding biocompatibility. Mechanical testing proved to have significantly better performance (stiffness, strength) than many known thermoplastic biopolymers.

Keywords: biocompatibility; bone tissue engineering; cell proliferation; mechanical properties; osteoblast; photopolymerization; rapid prototyping

1 Introduction

Autografts, tissue obtained from another site in the same subject of the same species, are the gold standard for tissue repair and substitution. However, the use of autografts has some serious disadvantages, such as additional expense and trauma to the patient, possibility of donor site morbidity, and limited availability. In the case of allografts, in addition to limited supply and high costs, other complications such as viral transmission and immunogenicity are of serious concern. Therefore, there is a critical need to develop bone substitute materials approximating the properties of tissue, which should be replaced, but without the drawbacks of autografts or allografts. In order to fulfill all requirements for replacement, a bone substitute must be biocompatible, meaning it must not be toxic or mutagen and it should be osteoconductive, meaning it should support the growth and proliferation of the cells of the specific tissue. Moreover, it is critical, that the scaffold supports the differentiation of the cells into the desired phenotype (1). It is also desirable that the scaffold is dismantled after implantation and is replaced by new tissue. Usually, the destruction of foreign material is performed by macrophages, which are also responsible for the inflammation process. These processes could result in repelling reactions and, therefore, the scaffolds must not be inflammatory (2). Furthermore, it is advantageous that the replacement material is dismantled by the natural process, the resorption that is performed by the osteoclasts. Therefore, special attention should be drawn to the fact that the material induces osteoclastogenesis.

Degradable polymers that are already in clinical use are usually based on polyesters such as poly(ε-caprolactone) or poly(α-hydroxy acids) (e.g. copolymers of lactic and glycolic acid). These polyesters cannot be used in the case of larger defects, e.g. after removal of a bone tumor, because of their hydrolytic degradation, which causes a rapid loss in mechanical strength. Moreover, the locally high concentration of free acids can result in tissue necrosis.

For tissue engineering, these polymers are processed by different melt or solution techniques based on Rapid Prototyping (e.g. Fused Deposition Modeling, 3D-Printing or Selective Laser Sintering), however, all of them suffer from insufficient resolution or time-consuming shaping processes. Of significant importance for clinical use are

Address correspondence to: R. Liska, Institute of Applied Synthetic Chemistry – Division of Macromolecular Chemistry, Vienna University of Technology, Getreidemarkt, 9/163/MC A-1060, Vienna, Austria. E-mail: rliska@otech7.tuwien.ac.at

ceramic-based bone replacement materials. These materials can be provided as foam-like structure or as flakes, respectively powders. The utilized ceramic component of these materials is frequently of bovine origin. Alternatively, chemically synthesized calcium-phosphate-based ceramics are utilized. Due to their excellent bioactivity, bioglasses have found widespread application. The main drawback of these materials is low strength due to their low fracture toughness. Alternative techniques are injectable bone cements, which solidify *in vivo*. These materials suffer from the fact that the polymerization heat can cause tissue necrosis and the resulting implant is not porous, which limits the movement of cells and diffusion of nutrients into the matrix. Large bony defects still pose a significant problem in orthopedic, as well as craniofacial surgery. Since these defects which may be caused by trauma, tumor, etc. differ in size, shape and location, it is necessary to develop a technique where a bone substitute can be made in any form or shape.

Stereolithography seems to be a suitable processing technique for larger bone replacement materials. Direct fabrication (3), of cellular structures with high resolution made out of a photocurable liquid acrylate-based formulation, that cures by radical polymerization, is possible. Indirect approaches are also viable where a sacrificial mold is made by RP (4, 5). This mold is then filled with a thermosetting polymer, and afterwards removed thermally or by using appropriate solvents. Since the materials generally used as biopolymers are thermoplastic polyesters, they are not suitable for the fabrication of bone replacement materials by stereolithography. Only a few papers were published that focus on photopolymerizable monomers that lead to biocompatible and biodegradable polymers. For example, poly(propylene fumarate) has often been described, and can be photocrosslinked with diethyl fumarate. Beside low photoreactivity, the resulting polymers are not porous and far too soft for replacing bone (6–8). Block copolymers consisting of a central diethylene glycol segment, several units of lactic acid or ε-caprolactone terminated with (meth)acrylic moieties (9–11) or a photopolymerizable lysine based monomer (12) gave promising results concerning cell adhesion and mechanical properties. New materials based on (meth)acrylate modified oligopeptides are expected to degrade by enzymatic degradation, which is slower than autocatalytic hydrolytic degradation of polyesters, and therefore provide longer mechanical support for regrowing bone (13). All these photopolymerizable polymers are solid and therefore are not useful alone for stereolithography. Liquid methacrylic anhydrides are also an important class of biodegradable monomers (14, 15).

In our present project, we aim at the development of such acrylate-based formulations for cellular implants, which can be photopolymerized directly by stereolithography or are suitable for thermal curing in molds. To tune the material properties regarding processability, biocompatibility as well as mechanical and degradation properties several components such as crosslinkers, reactive diluents, fillers and initiators have been considered. To overcome the problem of uncontrolled hydrolytic cleavage of ester containing monomers, biodegradability is introduced by multi-acrylated crosslinkers that can be cleaved enzymatically *in vivo*. Processing properties of the formulation and the network density of the polymer can be tuned by reactive diluents. Soluble filler materials are applied to tune the viscosity for an optimum resolution of the stereolithographic shaping process. Adequate photoinitiators, as well as fillers for advanced mechanical properties are also required.

In this paper, we discuss the selection and evaluation of different mono and multi-acrylated reactive diluents and suitable photoinitiators regarding photoreactivity. Mechanical properties and support for proliferation of osteoblast-like cells of these polymers will also be considered. Evaluation of special amide-based crosslinkers and fillers, as well as formulations for stereolithography will be discussed in future papers.

2 Experimental

2.1 Materials

All reagents, unless otherwise noted, were purchased from Sigma-Aldrich and were used without further purification. The monomers acrylic acid 2-(2-ethoxy-ethoxy)-ethyl ester (EEA), methacrylic acid 2-(2-ethoxy-ethoxy)-ethyl ester (EEM), acrylic acid 2-butylcarbamoyloxy-ethyl ester (BEA), methacrylic acid 2-hydroxy-ethyl ester (HEMA), and glycerol 1,3-diglycerolate diacrylate (GGA) were also obtained from Sigma Aldrich. N,N-Dimethyl-acrylamide (DMA) and acrylic acid (AA) were received from Fluka and N,N′-diethyl-1,3-propylenbisacrylamide (EPA) and 2-methyl-acrylic acid 2-{2,2,4-trimethyl-6-[2-(2-methyl-acryloyloxy)-ethoxycarbonylamino]-hexylcarbamoyloxy}-ethyl ester (UDMA) were obtained from Ivoclar Vivadent as a gift. Further monomers are: Tetraethyleneglycol diacrylate (E4-A, Sartomer), trimethylolpropane triacrylate (ETA, Cray Valley, Genomer 1330), ethoxylated trimethylolpropane triacrylate (TTA, Rahn, Sartomer 415, with 20 mol ethoxylated, MW 1176 g/mol) N,N-diisopropyl-acrylamide (DPA, Chemie Linz) and methacrylic acid (MA, Merck). N,N-Diisobutyl-acrylamide (DBA) was prepared as described (16). Photoinitiators Irgacure 819 (Bis(2,4,6-trimethylbenzoyl)-phenylphosphine oxide) and Irgacure 2959 (2-Hydroxy-1-[4-(2-hydroxyethoxy)phenyl]-2-methyl-1-propanone) were received from Ciba SC as a gift.

2.2 Differential Scanning Photocalorimetry

Differential scanning photocalorimetry (Photo-DSC) was conducted with a modified Shimadzu DSC 50 equipped with a home-made aluminum cylinder (height 6.8 cm). Filtered light (400–500 nm) was applied by a light guide (Efos-Novacure) attached to the top of the aluminum cylinder. The light intensity at the level of the surface of the cured samples was measured by an EIT Uvicure® high energy UV integrating radiometer. Irradiation was carried out for at

least 5 min. A light intensity of 30.16 mW/cm^2, which corresponded to 1500 mW/cm^2 at the tip of the light guide, was used. The measurements were carried out with 1 wt% of an equimolar mixture of camphorquinone (CQ) and N,N-dimethylaminobenzoic acid ethyl ester (DMAB) as initiator in an isothermal mode at room temperature under air atmosphere. The mass of the samples was 5 mg. The time to reach the maximum polymerization heat (t_{max}), the double bond conversion (DBC) and the maximum rate of polymerization (R_p) were determined.

2.3 Mechanical Testing

To investigate the mechanical properties of the selected polymers, dynamical mechanical analysis and bending strength tests were carried out. Therefore, test specimens (rods, 20 mm length, 3 mm width, 3 mm height) were made from the monomers with 1 wt% of an equimolar mixture of CQ and DMAB as initiator. Photocuring was performed with a high pressure mercury lamp (1000 W, distance 15 cm) under nitrogen atmosphere within 3–10 min depending on the type of monomer. Polymers from mono-acrylates were characterized in two ways. Homopolymers were prepared for the behavior of the pure polymer. A second set of experiments was carried out with 20 wt% of EPA as crosslinker. These copolymers were used for biocompatibility tests to avoid swelling and dissolution in the cell culture.

To determine the stiffness, the beams were placed in a dynamic mechanical analysis machine (TA Instruments DMA 2980) with a span-width of 20 mm. An extra initial load was applied in order to assure the direct contact between the sample and the clamp. The beams were tested with a frequency of 1.0 Hz in the temperature range between 10°C and 50°C. Typical curves obtained by this method are displayed in Figure 1.

The bending strength and the failure strain were measured with a universal tensile testing machine (Zwick Z050, Zwick/Roell). The maximal strain applicable in the middle of the beam was determined. A preload of 0.5 N was used and the velocity of the crosshead was 5 mm/min and 10 mm/min after 0.25% strain, respectively.

2.4 Biocompatibility

Test specimens were made from previously selected monomers to verify their biocompatibility. In the case of mono-acrylates, 20 wt% crosslinker EPA was added. In all cases, 1 wt% of an equimolar mixture of CQ and DMAB was used as the initiating system. The mixture was filled into a silicon mold (0.9 cm diameter, 0.15 cm height) and photocured with a high-pressure mercury lamp (1000 W, distance 15 cm) under nitrogen atmosphere. Depending on the type of monomer, the curing time was between 3 and 10 min. Afterwards, the test specimens were extracted with different organic solvents ($CHCl_3$, MeOH, EtOH), phosphate buffered saline (PBS) and water in an ultrasonic bath to remove residual monomer.

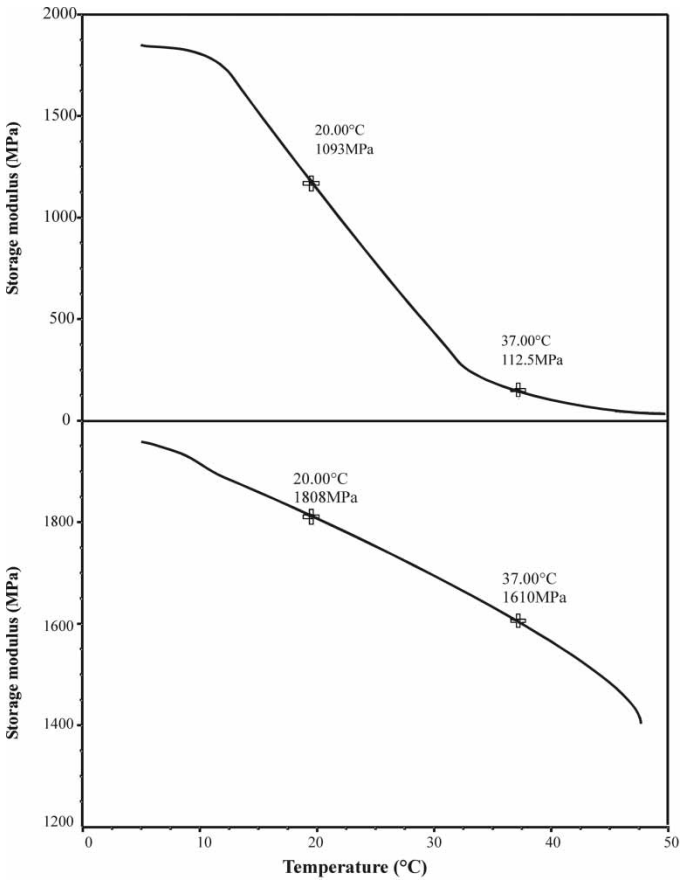

Fig. 1. Dynamic mechanical analysis (3-point bending) of BEA (top) and DBA (bottom) crosslinked with 20 wt% EPA.

To estimate whether osteoblasts accept the new polymers as growth support (biocompatibility), measurements of cell viability and multiplication of MG63 osteoblast-like cells with EZ4U (Biomedica, Austria) were used. This assay is based on the conversion of an uncolored tetrazolium salt into a formazan dye by the mitochondria of living cells.

The test specimens were placed into a multi-well plate and sterilized for 30 min in a distance of 14 cm with a 15 W UVB tube (Sylvana) on both sides. Thereafter, the space between the test specimen and the wall of the well were closed with agarose, cells were seeded at a density of 50,000 cells/cm^2 in αMEM supplemented with 5% FBS, 4.5 g/l glucose and 30 μg/ml gentamycin, and cultured for three days in a humidified air under 5% CO_2 at 37°C. Then, a change to fresh culture medium was performed and after one hour, the assay mixture was added. After a further 3 h culture period, the color of the medium was measured in a microplate reader at 492 nm against 620 nm. The measured extinction was converted to cell number by a calibration curve performed in separate experiments. Statistical analyses were performed by ANOVA with Bonferroni's multiple comparison

test using Prism 4 (GraphPad Software Inc. CA) and $P \leq 0.05$ was considered to be significant.

3 Results and Discussion

Different commercially available monomers, either mono-acrylates (Figure 2) or multi-substituted monomers (Figure 3), were investigated concerning reactivity, mechanical properties and biocompatibility. Selection of monomers was carried out under consideration of different functional groups (-COOH, -OH, -OCONH- and oligo (ethylene glycol)). Additionally, hydrolysable esters based on acrylates and methacrylates and more stable acrylamides were investigated. Mechanical properties are expected to be tuned by hydrogen bond formation of functional groups and by network density using mono-or multi-acrylated monomers. Biocompatibility and biodegradability cannot be classified in that manner, and are more related to the structure of the entire building block and the mechanics of the polymer (17).

HEMA has often been described as a biocompatible photopolymer and is applied for contact and intraocular lenses (18). Acrylic and methacrylic acid were selected because polymers thereof can be considered as degradation products of most esters (e.g. from EEA, EEM, BEA, and HEMA). Generally, less is known on acrylamides and therefore DPA, DBA and DMA were investigated.

In the case of difunctional monomers, EPA and UDMA are well known from dental applications, giving polymers with outstanding mechanical properties. E4-A and ETA are not known to give hard polymers due to the flexible oligoethylene glycol spacers with excellent biocompatibility, but have a poor tendency for cell adhesion. TTA and GGA have not been evaluated so far.

3.1 Photoreactivity

Beside biocompatibility and mechanical properties, photoreactivity is an important selection criterion for the monomers because of sufficient double bond conversion, and in the case of direct printing, short building times for rapid prototyping are desired. Differential scanning photocalorimetry (Photo-DSC) is a unique method for the fast and

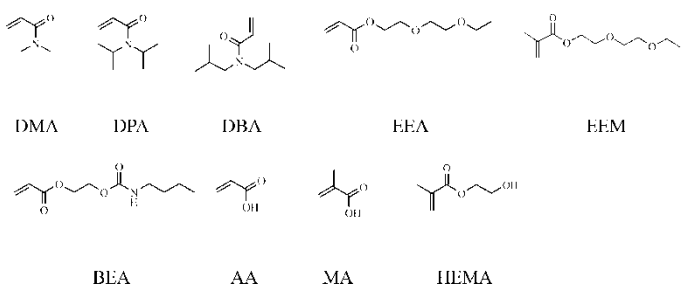

Fig. 2. Mono-acrylated monomers.

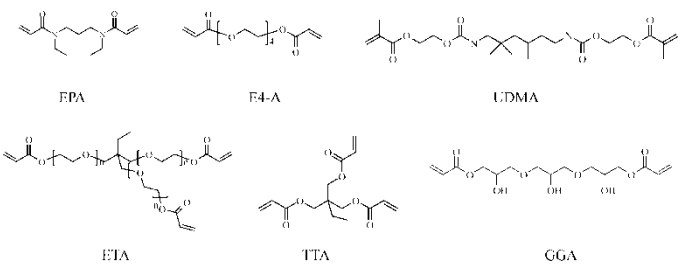

Fig. 3. Multi-acrylated monomers.

accurate evaluation of the reactivity of monomers. Various important parameters are obtained with one single measurement. The time to reach the maximum heat of polymerization (t_{max}) is a parameter which depends on photoreactivity and inhibition period. Total DBC was calculated from the overall heat evolved (ΔH_p), where $\Delta H_{0,P}$ is the theoretical heat obtained for 100% conversion (19) (Equation (1)).

$$DBC = \frac{\Delta H_P \times M}{\Delta H_{0,P}} \tag{1}$$

Initial rates of polymerization R_p [mol L^{-1} s^{-1}] were calculated from the height of the maximum of the plots h [mW/mg] and the density of the monomer ρ [19] following Equation (2).

$$R_P = \frac{h \times \rho}{\Delta H_{0,P}} \tag{2}$$

In the present studies, the Photo-DSC measurements were carried out at room temperature with filtered light (1500 mW/cm^2; 400–500 nm) applied by a light guide (Efos-Novacure) using 1 wt% of an equimolar mixture of CQ/DMAB as photoinitiator (PI). This combination is well known from dental applications and has been described to be exceptionally biocompatible (9).

The photo-DSC data of the mono-acrylates are shown in Figure 4. As expected, acrylates and acrylamides gave significantly higher R_p and lower t_{max} than methacrylic compounds. Small monomers like AA and DMA showed higher values for the R_P than monomers with higher molecular weight. The exceptional low reactivity of acrylamide DPA can be assigned to sterically demanding substituents, the isopropyl groups. Within the acrylates, sterical effects and functional groups also play an important role on the polymerization rate. High R_p and DBC of BEA and HEMA in the group of acrylates and methacrylates, respectively might be assigned to pre-organization by hydrogen bonding (20).The extremely low DBC of (meth)acrylic acids AA and MA could be explained by precipitation of the formed polymer thus terminating propagation reaction.

Figure 5 shows the photo-DSC data of the multi-acrylated monomers. As expected, multi-substituted monomers yielded lower DBC than mono-acrylates due to the network formation. In most cases, sufficient R_P and excellent t_{max} were observed, thus making them all suitable from the viewpoint

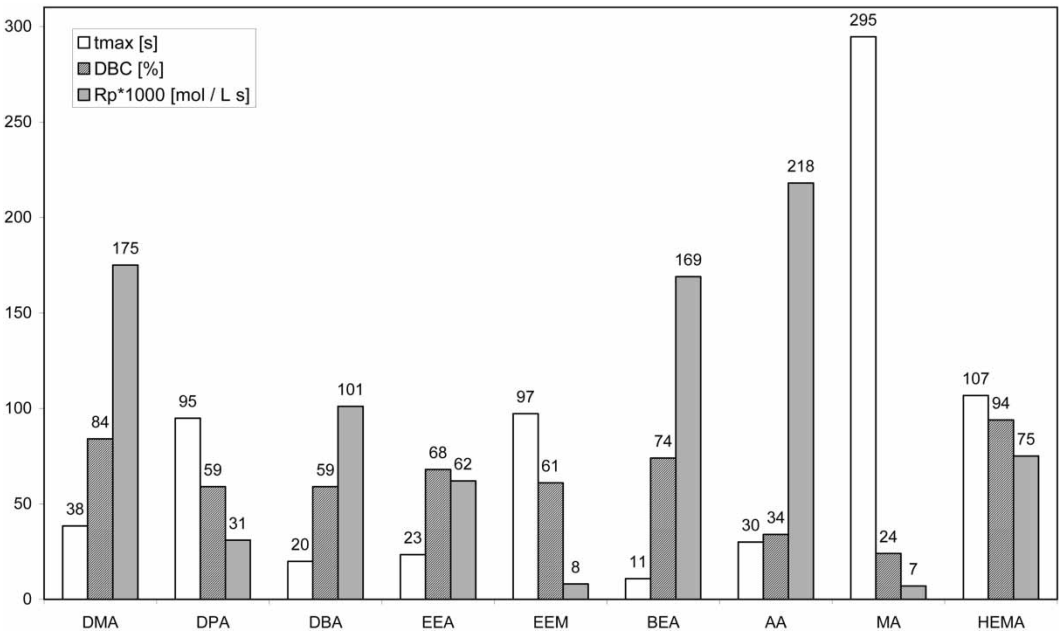

Fig. 4. Photo-DSC data of mono-acrylated monomers.

of reactivity. Generally, low t_{max} compared to mono-acrylated monomers can be explained by the gel effect. Excellent photopolymerization behavior of E4-A can be assigned to the flexible spacer. Comparably low photoreactivity of EPA can be explained by the low molecular weight and less flexibility of the monomer, thus giving rigid and tight networks. Low R_p of ETA compared to TTA can be assigned to the high molecular weight of the monomer.

The photoinitiating system consisting of CQ and DMAB was selected for the preparation of test specimens because of its known biocompatibility and the suitability for the curing of thick layers due to the photobleaching effect (21). Due to the bimolecular Type II mechanism, the polymerization rate might be too low for an application in rapid prototyping. Therefore, two α-cleavable Type I photoinitiators and the new DPD (Figure 6) were tested for their applicability in a

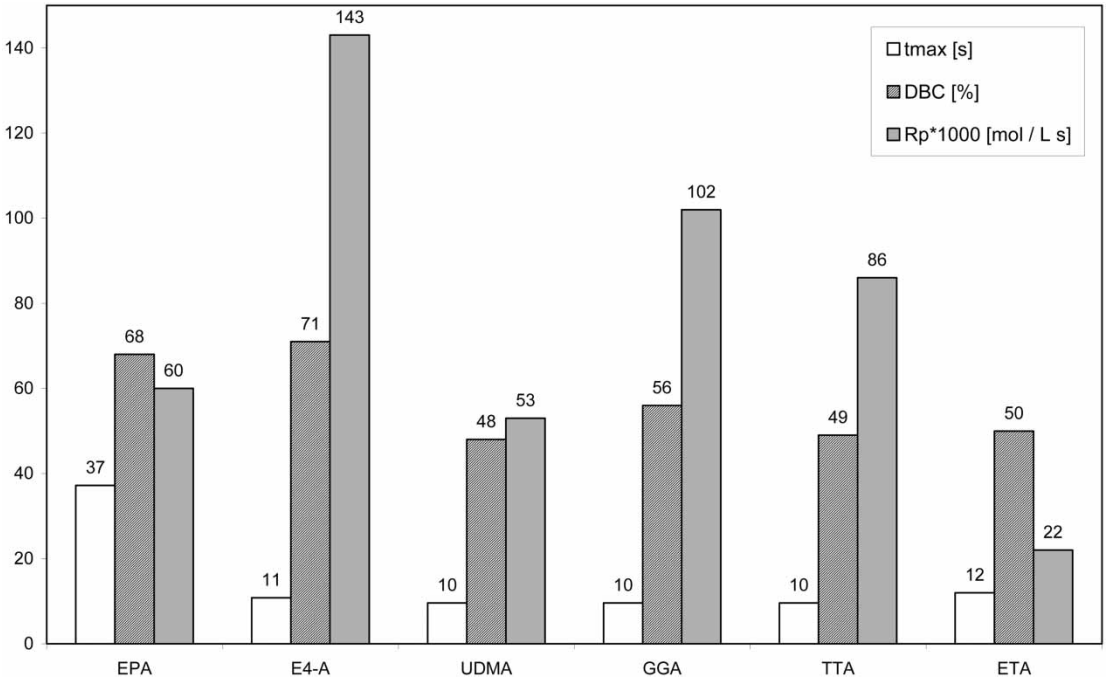

Fig. 5. Photo-DSC data of multi-acrylated monomers.

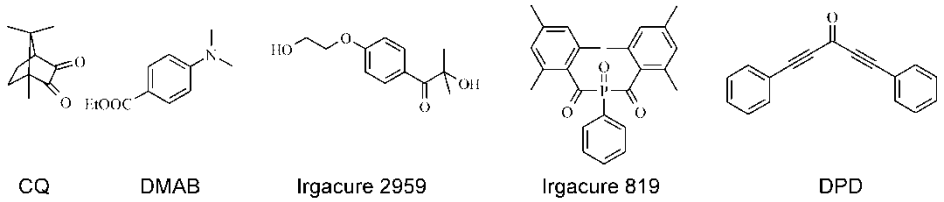

Fig. 6. Structure of photoinitiators, CQ/DMAB, Irgacure 2959, Irgacure 819 and DPD.

biodegradable tissue scaffold. The bisacylphosphine oxide Irgacure 819 is a very promising candidate for rapid prototyping due to its high reactivity and its absorption tailing out in the visible region. This photoinitiator is ideally suitable for the rapid prototyping process using the DLP principle (3) with light emission only in the visible region. The initiator has already found widespread application in dental materials (22), but not yet in biodegradable systems. The hydroxyalkylphenone Irgacure 2959 has often been used for photocuring of biopolymers (23) and the recently described DPD was also of interest because of the low toxicity (LD50 >1 g/kg (24)). Because of the absorption below 400 nm, the application of these two initiators is limited to rapid prototyping machines with appropriate UV-lasers. Photo DSC was used to compare the efficiency of the photoinitiators. Therefore, 0.5 wt% of Irgacure 819 and Irgacure 2959, respectively, and 1 wt% of an equimolar mixture of CQ and DMAB were dissolved in EPA and measured with filtered light (320–500 nm, 1500 mW/cm^2). Due to the high extinction coefficient of DPD only 0.3 wt% was necessary. Results from the photo-DSC experiments are given in Table 1. Using this method of analysis, the advantages of curing with Irgacure 819 as photoinitiator are clearly visible. Exceptional high DBC is of significant importance for low migration systems. Generally, the time for entire curing is very similar for all photoinitiators as the values for t_{max} show. Under practical conditions the available light source wavelength is responsible for the selection of the photoinitiator.

3.2 Mechanical Properties

In order to evaluate the mechanical properties of the materials, 3-point bending tests were performed to measure the strength. DMA measurements (also in 3-point bending) were used to measure the elastic modulus of the materials and its temperature dependency.

Polymers from mono-acrylated monomers were tested with 20 wt% ETA as crosslinker- that was necessary to enable biocompatibility tests in aqueous culture medium-but also without crosslinker to measure the original (intrinsic) mechanical properties. As shown in Tables 2, 3 and Figure 7 the mechanical properties of the tested biopolymers vary significantly. Some materials were immeasurable due to their rubber-like texture, e.g., polymers from BEA, EEA, EEM (Table 2) and ETA (Table 3, Figure 7). This can be attributed to the soft and flexible side chains based on poly(ethylene glycol). Polyurethanes also belong to the class of soft and flexible polymers.

In comparison with traditional (bio)polymers (see Table 4), some of the polymers described in this work exhibit excellent strength and stiffness values. The summarized data on mechanical properties (Table 2, Table 3 and Figure 7) can be used

Table 1. Photoreactivity of photoinitiators

Photoinitiator	t_{max} [s]	DBC [%]	$R_P^* \cdot 10^3$ [mol L^{-1} s^{-1}]
Irgacure 819	7,8	87	227
Irgacure 2959	12,6	74	141
CQ/DMAB	13,2	63	102
DPD	13,2	62	93

Table 2. Mechanical properties (storage modulus) of homopolymers measured by dynamic mechanical analysis (DMA) in 3-point bending modus. Mono-acrylated monomers were also tested with 20 wt% of crosslinker EPA.

	Storage modulus, 20°C		Storage modulus, 37°C	
Material	Homopolymer [MPa]	+20 wt% EPA [MPa]	Homopolymer [MPa]	+20 wt% EPA [MPa]
DMA	Too soft	2900	Too soft	2690
DPA	ncsm[a]	880	ncsm[a]	757
DBA	1380	1810	1220	1610
EEA	Too soft	42	Too soft	38
EEM	Too soft	Too soft	Too soft	Too soft
BEA	Too soft	1090	Too soft	113
AA	5280	4920	4810	4620
MA	ncsm[a]	ncsm[a]	ncsm[a]	ncsm[a]
HEMA	2650	1550	2140	2390
EPA	3250	—	2830	—
E4-A	441	—	94	—
UDMA	2880	—	1590	—
GGA	2210	—	1710	—
TTA	2010	—	1660	—
ETA	Too soft	—	Too soft	—

[a]ncsm - no compact specimen manufacturable.

Table 3. Mechanical properties of homopolymers characterized by 3-point bending strength and failure strain. Mono-acrylated monomers were also tested with 20 wt% of crosslinker EPA.

	3-Point bending strength		Failure strain	
Material	Homopolymer [MPa]	+ 20 wt% EPA [MPa]	Homopolymer [%]	+20 wt% EPA [%]
DMA	26	55		
DPA	ncsm[a]	35	ncsm[a]	8.7
DBA	30	51	3.84	4.9
EEA	Too soft	Too soft	Too soft	Too soft
EEM	Too soft	Too soft	Too soft	Too soft
BEA	Too soft	Too soft	Too soft	Too soft
AA	70	93	9.6	6.9
MA	ncsm[a]	ncsm[a]	ncsm[a]	ncsm[a]
HEMA	74	96	5.1	14.0
EPA	42	—	2.3	—
E4-A	8	—	14.9	—
UDMA	87	—	12.2	—
GGA	45	—	14.4	—
TTA	54	—	4.5	—
ETA	Too soft	—	Too soft	—

[a]ncsm – no compact specimen manufacturable.

to study several parameters which influence the mechanical properties:

1. Some of the polymers (e.g. from AA) have excellent mechanical properties in a dry state, but due to swelling in aqueous media they quickly lose strength and even disintegrate after longer exposure to water.
2. In nearly all cases, crosslinked polymers perform better (as expected) regarding strength and stiffness compared to polymers from pure mono-acrylated monomers and, therefore linear polymers.
3. The temperature dependence of the mechanical properties is of importance since for most applications the biopolymers will be used at 37°C. Some of the investigated polymers (e.g. from UDMA) exhibit excellent stiffness values at room-temperature, but quickly soften at slightly elevated temperatures if the glass transition point is close or within the investigated temperature range. Main reasons for the softening at higher temperatures are probably hydrogen bonds which tend to break even at mild temperatures due to their low bond energy.
4. Additional effects like hydrogen bonds (e.g. polymers from UDMA, GGA) or a tight network of crosslinks (e.g. polymers from EPA, TTA) can increase the mechanical performance, even in the case of long and flexible side-chains. Therefore, significant weaker mechanical properties were observed in the case of polymers from E4-A and ETA.
5. Promising materials (from a biocompatibility, as well as from a mechanical point of view) include polymers from UDMA, GGA and TTA. All these materials exhibit strength and stiffness values comparable to or beyond commonly used biopolymers (see Table 4). Due to their high density of crosslinks and numerous hydrogen bonds polymers from UDMA and GGA become fairly tough, which is shown in their quite high elongation at break (see Table 3).

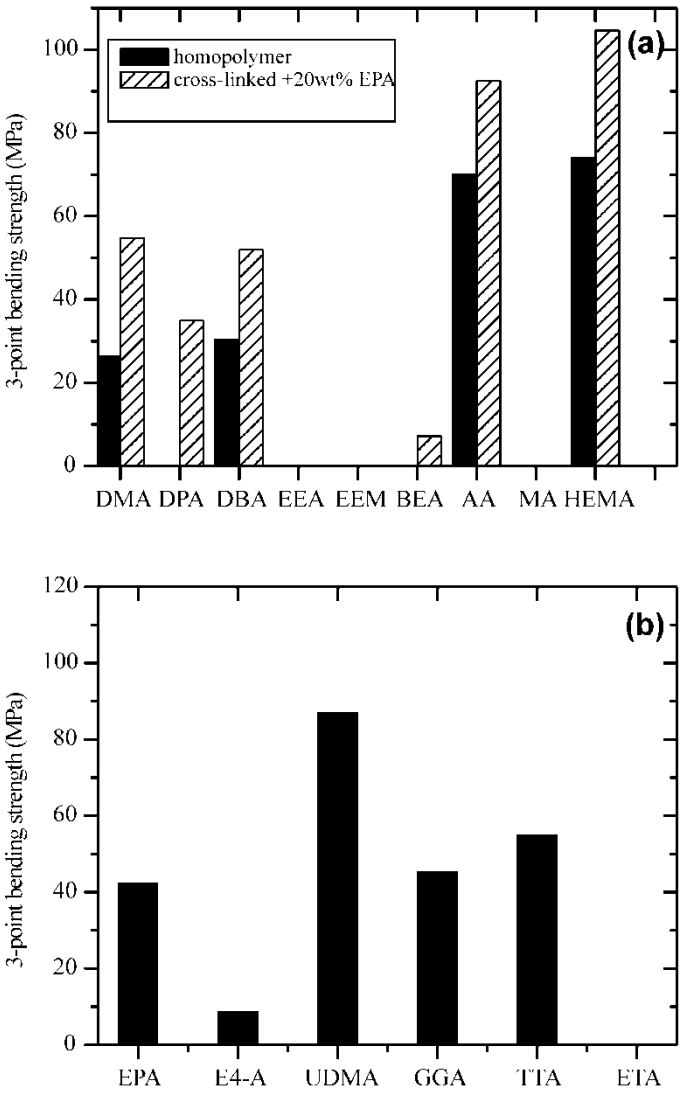

Fig. 7. 3-Point bending strength of polymers from (a) mono-acrylated and (b) multi-acrylated monomers. Empty values indicate that the material was not strong enough for a valid measurement.

3.3 Biocompatibility

The mono-acrylated monomers DPA, EEA, EEM, and BEA were crosslinked with 20 wt% of EPA and used for preparing test specimens for biocompatibility tests. To these samples, MG-63 osteosarcoma cells were seeded and cultured for 3 days. After this period, estimation of the cell number on these resins did not show significant differences; only the polymer made from DBA yielded a significant higher cell number (160%, Figure 8). The superior support of DBA compared to DPA for cell multiplication could originate

Table 4. Mechanical properties of common polymers and biomaterials. The values for PE, PA and POM were obtained from the Cambridge Engineering selector (Granta Design)

Material	Strength [MPa]	Young's modulus [MPa]
Polyamide (PA)	90	2800
Polyethylene (PE)	25	500
Polylactic acid (PLA) (32)	50	3500
Polycaprolactone (PCL) (33)	17	318
Polyoxymethylene (POM)	90	2900
Compact bone (34)	50–150	11000

from a better adsorption of the serum proteins of the culture medium. This may be due to a more readily accessibility of the amino-group of DBA, which is known for better cell adhesion and osteoblastic differentiation (25, 26). The sterical hindrance of the isopropyl group in DPA has already been seen in the low photopolymerization activity. On the HEMA made polymer, after 3 days of culture only about 50,000 cell per well could be found; this were less cells than seeded (Figure 8). This could mean that on this material either fewer cells adhered without further multiplication or cells were dying. We suggest the first case because, although the material is known to be compatible with cell cultures, it does not support attachment of mammalian cells and is usually used to cover culture dishes to prevent cell adhesion (27). The hydroxyl-group of the ethylene glycol may be responsible for the low adhesion followed by a reduced cell number after the 3-days culture time (25). The polymers formed from DMA, AA and MA, each with 20 wt% EPA as crosslinker, were not stable in cell culture and could not be tested. Therefore, new test specimens with

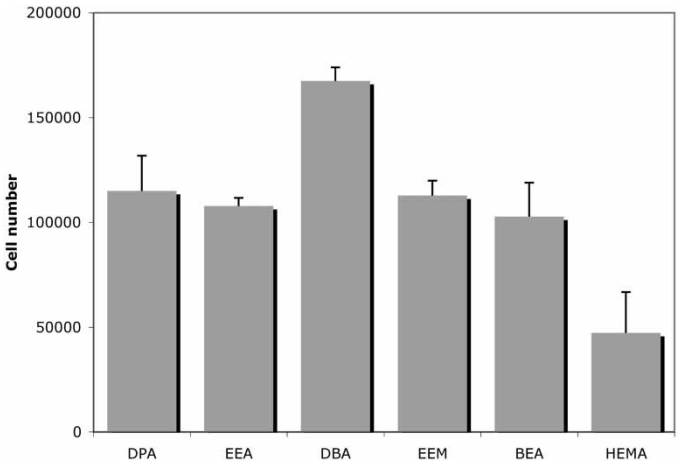

Fig. 8. Cell number on polymers made from mono-acrylated monomers crosslinked with 20 wt% EPA after 3 days of culture. Bars represent mean ± SD. n = 4; DBA and HEMA vs. all other resins: $p \leq 0.01$.

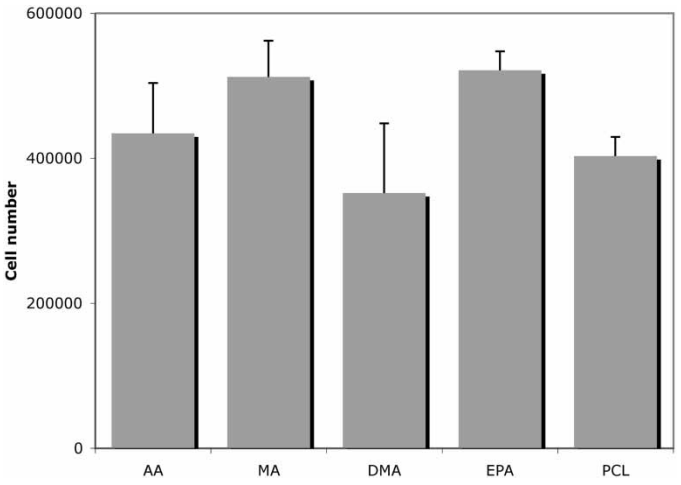

Fig. 9. Cell number on polymers made from mono-acrylated monomers AA, MA, and DMA with 80 wt% crosslinker EPA after 3 days of culture in comparison to PCL and polymer from EPA. Bars represent mean ± SD. n = 4.There were no significant differences between the cell numbers on the resins.

80% crosslinker EPA and 20% mono-acrylated monomer were prepared. Figure 9 shows the cell number after 3 days of culture on polymers made from those monomers compared to polymers from EPA (crosslinker) and poly(ε − caprolactone) (PCL), a material already in clinical use. Test specimens made from MA and EPA were only marginally better in supporting cell multiplication than both made from DMA and PCL. However, there were no significant differences. The lack of distinct differences between AA, MA and DMA compared to EPA indicates that the crosslinker defines the biocompatibility of the polymers.

Distinct differences in cell number after 3 days of culture were found between the polymers made from multi-acrylated monomers (Figure 10). The low cell number on the polymer made of ETA may result from the numerous ethylene glycol moieties. Recently, it was demonstrated that increasing concentration of poly(ethylene glycol) in a backbone of tyrosine-derived polycarbonate resulted in a decrease of protein (fibronectin) adsorption followed by a decrease of cell adhesion (28). In GGA, which has a tri(glycerol) chain between the two acrylic moieties (Figure 3), there is a lower molar concentration of the critical ether group that could result in better support of both cell adhesion and multiplication (Figure 10). Furthermore, the free hydroxyl-group could support synthesis of bone proteins (25) that could increase the proliferation rate of the adhered osteoblasts.

Superior in the group of polymers made from multi-acrylated monomers and better than that made from TTA, is only the one made from UDMA, an urethane derivative (Figure 3), which is known to have high biocompatibility (Figure 10). Nearly as good as the urethane-derivative UDMA, was the until now unexplored TTA, a triacrylate. This resin was also superior in a direct comparison to a well-known polymer (E4-A) used for hydrogels (29) and

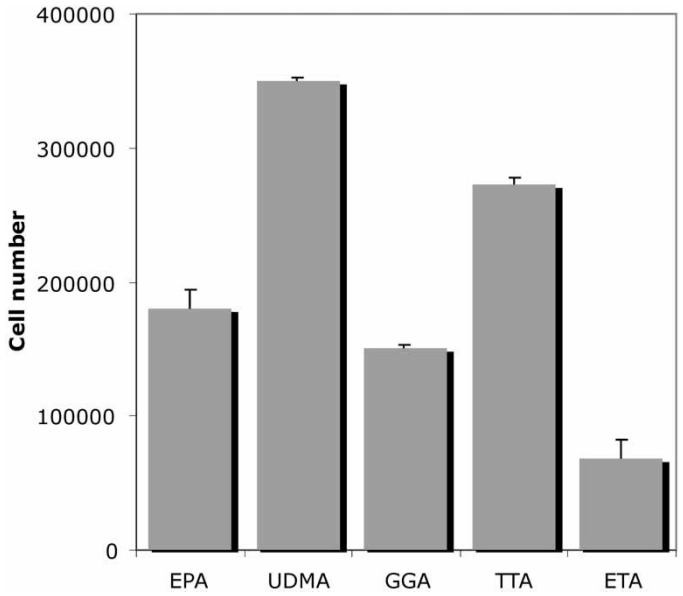

Fig. 10. Cell number on polymers made from multi-acrylated monomers after 3 days of culture. Bars represent mean $\pm$SD. n = 2; UDMA vs. EPA $p \leq 0.05$; GGA vs. UDMA $p \leq 0.05$; ETA vs. UDMA $p \leq 0.01$; ETA vs. TTA $p \leq 0.05$.

the polyester PCL that is used for clinical applications (Figure 11). In addition to the cell proliferation and viability studies, the morphological appearance of the cells on the best two polymers, TTA and UDMA, were investigated by staining the stress fibers with phalloidin and investigation by confocal microscopy. On glass, osteoblastic MG-63 cell showed the typical cubical appearance with well-established stress fibers and distinct adhesions points to the substratum (Figure 12-A). Cells cultured on UDMA displayed a rhomboid appearance with strong stress fibers and distinct

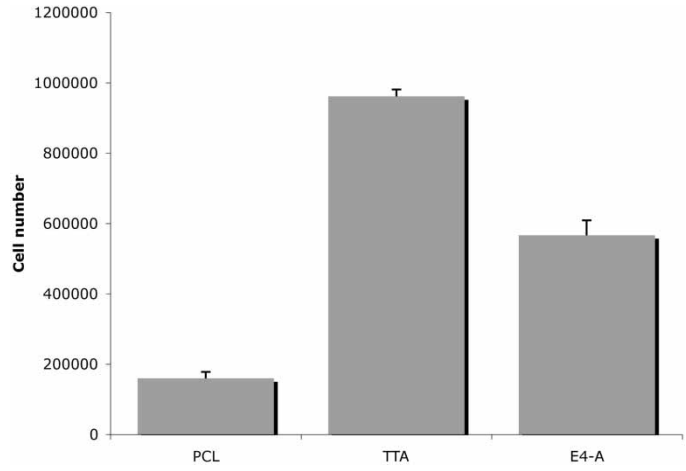

Fig. 11. Comparison of cell multiplication after 3 days of culture on a commercial (PCL) and polymers from E4-A and TTA. Bars represent mean $\pm$SD. n = 3; PCL vs. TTA, E4-A, $p \leq 0.001$. TTA vs. E4-A, $p \leq 0.001$.

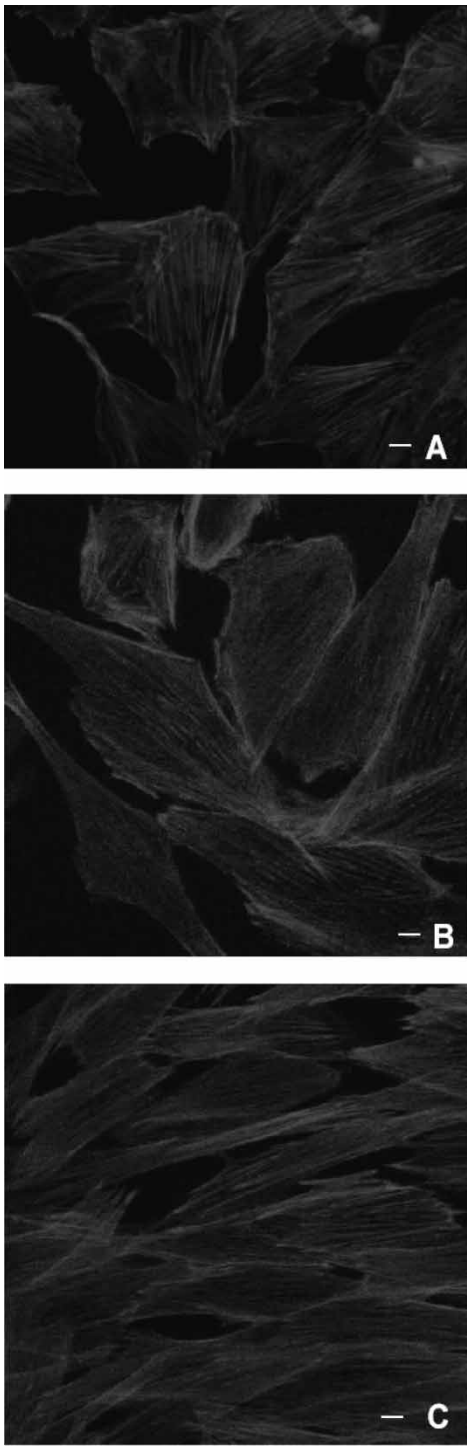

Fig. 12. Morphology and stress fibers of MG-63 osteosarcoma cells cultured on glass (A) UDMA (B) and TTA (C).

Cells were seeded and cultured for 3 days and after fixation stained with phalloidin-TRITC. Pictures were taken with a confocal laser scanning microscope (Leica TCS4D; Scale bar 10 μm).

Note that cells in all tested materials form strong stress fibers and well established focal contacts. Although, cells grown on glass had a cubical appearance as typically found for osteoblasts, while on TTA they have a fibroblast-like appearance. On UDMA the cells looked in-between cubical and fibroblastic.

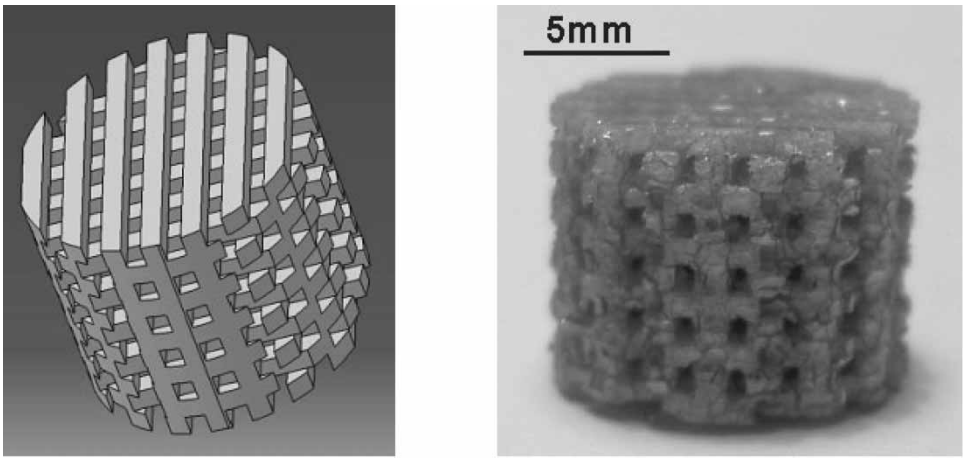

Fig. 13. Three dimensional structures made by rapid prototyping. The left image is a view of the original CAD structure. The right image shows the corresponding scaffold obtained by casting an EPA-based polymer into a cellular wax mold.

adhesion structures as well (Figure 12-B). The morphology of the cells cultured on TTA (Figure 12-C) was slightly longer compared to the cells on the other materials, and their appearance showed a fibroblastic character. However, stress fibers and contacts to the substratum were well established. The different morphology of the cells could indicate that during the culture period the cells did not reach the same differentiation status. This could mean that the substratum influences the development of the cells indicated by different morphological appearance. This could further result in differences of protein synthesis as recently found with osteoblast-likes MC3T3-E1 on self-assembled monolayers with well defined chemistries as model biomaterial surfaces (25). Further experiments will show whether the appearance of the cells correlates with the differentiation status e.g. glass grown cells are more differentiated (cubical shape) than on TTA (fibroblast like shape).

From these sets of experiments, it can be concluded that the presence of a single functional group does not control the cell adhesion and cell multiplication behavior, but rather the whole structure of the monomer is responsible. Nevertheless, it seemed that ether groups, as well known from poor adhesion behavior from poly(ethylene glycols), but also hydroxy groups (GGA, HEMA) have no cell multiplication promoting influence. Carboxylic acids and ester groups, and especially amide linkages (DBA, EPA) as in proteins and urethane groups (UDMA) seemed to be preferred.

In an additional set of experiments, the biocompatibility of different types of photoinitiators in EPA was compared. Within the error of measurements, hydroxyalkylphenone *Irgacure 2959, DPD* and surprisingly, also the bisacylphosphine oxide based PI *Irgacure 819* gave very similar cell numbers as the well known system consisting of CQ and DMAB (data not shown).

In summary, we evaluated new monomers capable for rapid prototyping, which were superior to known polymers in supporting cell multiplication of human osteoblasts.

3.4 3D Scaffolds

The materials presented in this work have the potential for being shaped by rapid prototyping. For direct shaping by stereolithography further optimization has to be done regarding viscosity, UV-absorption and solubility of the polymer within the monomer by careful selection of crosslinkers, reactive diluents, photoinitiators and fillers (3). To obtain first 3D cellular parts, this optimization can be circumvented by using an indirect shaping process: EPA as resin was equipped with a thermal initiator (1 wt% benzoylperoxide and 0.2 wt% DMAB), which is well known to be biocompatible (30). A wax mold was fabricated using a RP machine (Solidscape/Modelmaker) (4, 31). The mixture was then cast into this mold, which was removed after the resin set (45°C; 24 h) by dissolving in ethanol. A sample part obtained by this technique is shown in Figure 13.

4 Conclusions

In the present paper, the evaluation of different mono and multi-acrylated monomers as reactive diluents for rapid prototyping of cellular bone replacement materials is presented. Photoreactivity was determined by photo-DSC and was found to be in most cases high enough for direct printing by stereolithography. Biocompatibility was tested with osteoblast-like cells. As expected, polyethylene glycol type monomers are not toxic, but show poor cell multiplication. Acrylates with urethane units and especially most dialkylacrylamide based monomers gave outstanding biocompatibility. Compared to usually applied PCL, polymer obtained from TTA gave more than 5-fold higher number of cell multiplication after 3 days of culture. Mechanical testing was carried out by determining the storage modulus and strength in 3-point-bending. As expected, small crosslinkers and monomers with hydrogen bonding capacity gave significantly better performance (stiffness, strength) than many known thermoplastic biopolymers.

5 Acknowledgment

Samples EPA and UDMA provided by IVOCLAR VIVADENT AG, photoinitiators from Ciba SC, and financial support by the "Austrian Nano Initiative" under contract no. N-703 is kindly acknowledged.

6 References

1. Niklason, L.E. and Langer, R. (2001) *Jama*, **285**(**5**), 573–6.
2. Blaine, T.A., Rosier, R.N., Puzas, J.E., Looney, R.J., Reynolds, P.R., Reynolds, S.D. and O'Keefe, R.J. (1996) *J. Bone Joint. Surg. Am.*, **78**(**8**), 1181–92.
3. Liska, R., Schwager, F., Cano Vives, R. and Stampfl, J. (2004) *Polymer Preprints*, **45**, 77–78.
4. Woesz, A., Rumpler, M., Manjubala, I., Pilz, C., Varga, F., Stampfl, J. and Fratzl, P. (2005) *Mater. Res. Soc. Symp. Proc.*, **874**(L7.9.1).
5. Liska, R., Schwager, F., Maier, C., Cano Vives, R. and Stampfl, J. (2005) *Journal of Applied Polymer Science*, **97**, 2286–2298.
6. Cooke, M., Fisher, J.P., Dean, D., Rimnac, C. and Mikos, A. (2003) *Journal of Biomedical Materials–Part B Applied Biomaterials*, **64**, 65–69.
7. He, S., Timmer, M.D., Yaszemeski, M.J., Yasko, A.W., Engel, P.S. and Mikos, A.G. (2001) *Polymer*, **42**, 1251–1260.
8. Jo, S., Engel, P.S. and Mikos, A.G. (2000) *Polymer*, **41**, 7595–7604.
9. Davis, K.A., Burdick, J.A. and Anseth, K.S. (2003) *Biomaterials*, **24**, 2485–2495.
10. Metters, A.T., Anseth, K.S. and Bowman, C.N. (2000) *Polymer*, **41**, 3993–4004.
11. Zeng-guo, F. and Sanping, Z. (2003) *Polymer*, **44**, 5177–5186.
12. Müh, E., Zimmermann, J., Kneser, U., Marquardt, J., Mülhaupt, R. and Stark, B. (2002) *Biomaterials*, **23**, 2849–2854.
13. Zimmermann, J., Bittner, K., Stark, B. and Mülhaupt, R. (2002) *Biomaterials*, **23**, 2127–2134.
14. Temenoff, J.S. and Mikos, A.G. (2000) *Biomaterials*, **21**, 2405–2412.
15. Xie, D., Chung, I., Puckett, A.D. and Mays, J.W. (2005) *J. Appl. Polym. Sci.*, **96**, 1979–1984.
16. Maier, L. (1973) *Helvetica Chemica Acta*, **56**, 1252–1257.
17. Yeung, T., Georges, P.C., Flanagan, L.A., Marg, B., Ortiz, M., Ming, W., Funaki, M., Zahir, N., Ming, W., Weaver, V. and Janmey, P.A. (2005) *Cell Motil Cytoskeleton*, **60**(**1**), 24–34.
18. Montheard, J.P., Chatzopoulus, M. and Chappard, D. (1992) *Journal of Macromolecular Science, Reviews in Macromolecular Chemistry and Physics*, **C32**, 1–34.
19. Brandrup, J., Immergut, E.H. and Grulke, E.A. In Polymer Handbook 4th Ed.; John Wiley & Sons Inc: New York, , 365–381, 1999.
20. Lee, T.Y., Roper, T.M., Jönsson, E.S., Guymon, C.A. and Hoyle, C.E. (2004) *Macromolecules*, **37**, 3659–3665.
21. Crivello, J. and Dietliker, V. In Chemistry and Technology of UV-EB Formulation for Coatings, Inks and Paints; Bradley, G. Sita Technology Ltd: London; Vol. 3, 268, 1998.
22. Schmitt, W., Jochum, P. and Ellrich, K. (1989) Ger Offen DE 3801511.
23. Williams, C.G., Malik, A.N., Kim, T.K., Manson, P.N. and Elisseeff, J.H. (2005) *Biomaterials*, **26**, 1211–1218.
24. Kolyagina, G.F., Glazunova, N.P., Meshcheryakov, V.I., Gavrilov, L.D. and Vereshchagin, L.I. (1981) *Pharmaceutical Chemical Journal*, **15**, 46–50.
25. Keselowsky, B.G., Collard, D.M. and Garcia, A.J. (2004) *Biomaterials*, **25**(**28**), 5947–54.
26. Keselowsky, B.G., Collard, D.M. and Garcia, A.J. (2005) *Proc. Natl. Acad. Sci. U S A*, **102**, 5953–5957.
27. Fukazawa, H., Nakano, S., Mizuno, S. and Uehara, Y. (1996) *Int. J. Cancer*, **67**(**6**), 876–82.
28. Tziampazis, E., Kohn, J. and Moghe, P.V. (2000) *Biomaterials*, **21**, 511–520.
29. Liu, V.A. and Bhatia, S.N. (2002) *Biomedical Microdevices*, **4**, 257–266.
30. Lewandrowski, K.U., Gresser, J.D., Wise, D.L., White, R.L. and Trantolo, D.J. (2000) *Biomaterials*, **21**, 293–298.
31. Manjubala, I., Woesz, A., Pilz, C., Rumpler, M., Fratzl-Zelman, N., Roschger, P., Stampfl, J. and Fratzl, P. (2005) *Journal of Materials Science: Materials in Medicine*, **16**, 1111–1119.
32. Kasuga, T., Ota, Y., Nogami, M. and Abe, Y. (2001) *Biomaterials*, **22**(**1**), 19–23.
33. Koenig, M.F. and Huangt, S.J. (1995) *Polymer*, **36**(**9**), 1877–1882.
34. Gibson, L. and Ashby, M.F. In Cellular Solids–Structures and Properties 2nd Ed.; University Press: Cambridge, UK, 1997.